

Appendix A for

“Formation of bonanza Au-Ag-telluride ores in epithermal systems: Constraints from Cu-O isotopes and modeling”

Shen Gao^{1,2,*}, Albert H. Hofstra³, Kezhang Qin^{4,5}, Xinyu Zou⁴, Hong Xu²

¹State Key Laboratory of Geological Processes and Mineral Resources, China University of Geosciences, Beijing 100083, China

²School of Earth Sciences and Resources, China University of Geosciences (Beijing), Beijing 100083, China

³U.S. Geological Survey, P.O. Box 25046, Denver, CO 80225, USA

⁴State Key Laboratory of Lithospheric and Environmental Coevolution, Institute of Geology and Geophysics, Chinese Academy of Sciences, Beijing 100029, China

⁵College of Earth and Planetary Sciences, University of Chinese Academy of Sciences, Beijing 100049, China

Any use of trade, firm, or product names is for descriptive purposes only and does not imply endorsement by the U.S. Government.

Contents

Figures A1–A5.

Tables A1–A2.

References Cited

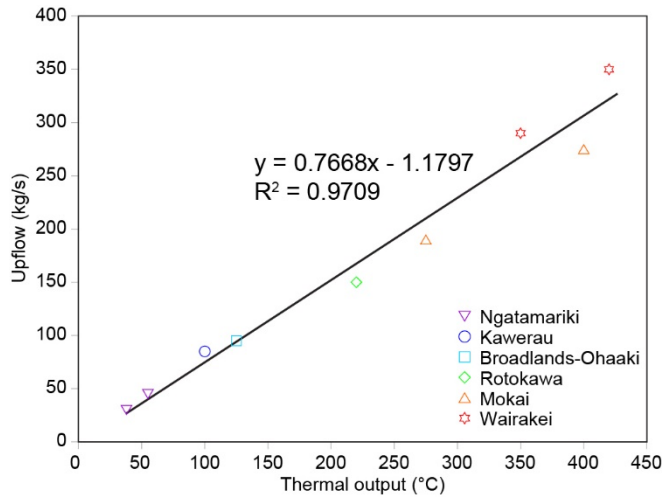


Fig. A1. Upflow vs. thermal output of modern geothermal systems (Data from [Simmons and Brown 2007](#)).

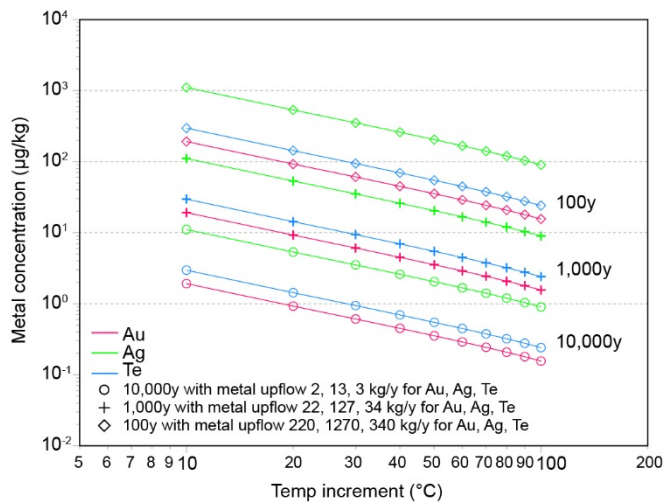


Fig. A2. Metal concentration vs. temperature increment from flux modeling.

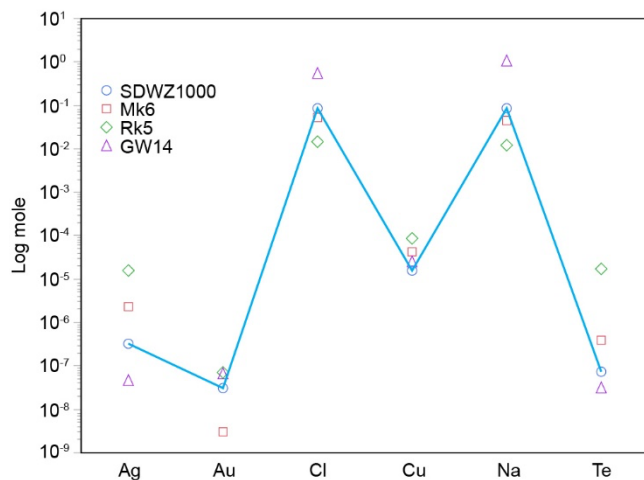


Fig. A3. Initial compositions at Sandaowanzi and compared with other Te-rich deep solutions (Data from [Simmons and Brown 2007](#)).

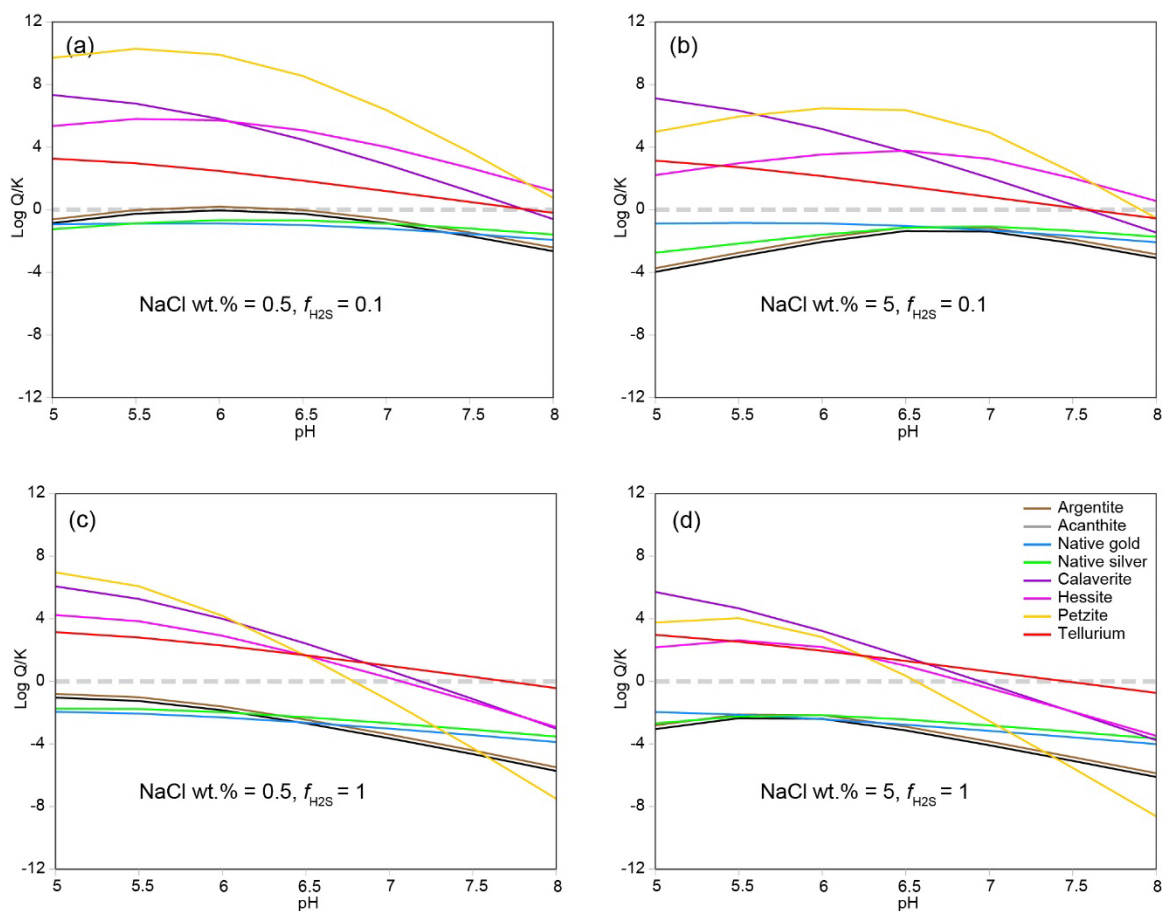


Fig. A4. Comparisons of physicochemical conditions in deep solutions. $T = 300\text{ }^{\circ}\text{C}$, $P = 86$ bars, $\text{H}_2\text{O} = 1\text{ kg}$, $f\text{CO}_2 = 1$, $\text{Log } Q/K(\text{quartz}) = 0$. The concentrations of Au, Ag, and Te are 6.09, 35.14, and 9.41 $\mu\text{g/kg}$, respectively, based on calculated values at $30\text{ }^{\circ}\text{C}$ intervals over a period of 1,000 years. The impact of salinity is minimal between 0.5 wt.% and 5 wt.%, and it is also less significant compared to the effects of $f\text{H}_2\text{S}$ and pH. The concentrations of CO_2 and SiO_2 were not evaluated in this study because of the presence of calcite and quartz precipitation in the veins, which have high concentrations of CO_2 and SiO_2 . The $\text{pH} = 8$ was chosen to maximize the solubility of Au, Ag, and Te in the solution. This pH value is also within the range typically found in Te-bearing geothermal systems (Simmons and Brown 2006). The concentrations of Cl^- and Na^+ were established using a 0.5 wt.% NaCl solution due to its low salinity (Table A2). Although $f\text{H}_2\text{S}$ is important, its concentration is typically low in modern geothermal systems (Simmons and Brown 2006; Simmons et al. 2016). The fugacity of H_2S was set at 0.2, within the range of 0.1 to 1. The saturation of CO_2 was used to fix HCO_3^- concentration, while quartz saturation was used to fix SiO_2 concentration.

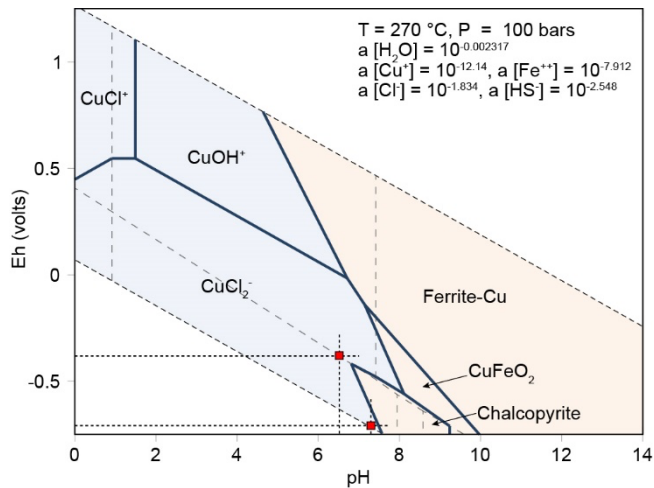


Fig. A5. Eh vs. pH plot at 270 °C from the mixing model. The red squares represent the Eh and pH ranges referred to in the mixing model.

Table A1. Metal concentrations from flux modeling.

Metal(loid)	Resource (kg)	Temperature increment (°C)	Thermal output	Upflow (kg/s)	Metal concentration (μg/kg)	Metal concentration (μg/kg)	Metal concentration (μg/kg)	Metal upflow (kg/y)	Metal upflow (kg/y)	Metal upflow (kg/y)
					10000y	1000y	100y			
Au	22000	10	49	36	1.92	19.17	191.69	2.2	22	220
		20	100	76	0.92	9.24	92.40			
		30	151	115	0.61	6.09	60.87			
		40	204	155	0.45	4.49	44.94			
		50	259	197	0.35	3.53	35.34			
		60	316	241	0.29	2.89	28.93			
		70	376	287	0.24	2.43	24.30			
		80	440	336	0.21	2.07	20.75			
		90	509	389	0.18	1.79	17.93			
		100	586	448	0.16	1.56	15.57			
Ag	127000	10	49	36	11.07	110.66	1106.56	1.27	127	1270
		20	100	76	5.33	53.34	533.40			
		30	151	115	3.51	35.14	351.39			
		40	204	155	2.59	25.94	259.40			
		50	259	197	2.04	20.40	203.99			
		60	316	241	1.67	16.70	167.01			
		70	376	287	1.40	14.03	140.25			
		80	440	336	1.20	11.98	119.78			
		90	509	389	1.03	10.35	103.49			
		100	586	448	0.90	8.99	89.86			
Te	34000	10	49	36	2.96	29.62	296.25	3.4	34	340
		20	100	76	1.43	14.28	142.80			
		30	151	115	0.94	9.41	94.07			
		40	204	155	0.69	6.94	69.45			
		50	259	197	0.55	5.46	54.61			
		60	316	241	0.45	4.47	44.71			
		70	376	287	0.38	3.75	37.55			
		80	440	336	0.32	3.21	32.07			
		90	509	389	0.28	2.77	27.71			
		100	586	448	0.24	2.41	24.06			

Table A2. Composition of the initial solution used for geochemical modeling.

Initial composition	Determined by	SDWZ deep H ₂ O	Heat H ₂ O
T = 300 °C	SIMS oxygen isotope	300	250
pH	Au, Ag, and Te dissolved	8	6.45
H ₂ O	1 kg solution	1 kg	1 kg
Cl ⁻	0.5 wt.% NaCl	8.56E-02	3.34E-02
SO ₄ ²⁻			1.17E-03
HCO ₃ ⁻	$f\text{CO}_2 = 1$		5.19E-01
HS ⁻	$f\text{H}_2\text{S} = 0.2$		
SiO _{2(aq)}	Quartz saturated		8.29E-03
Ca ²⁺			1.62E-04
Mg ²⁺			8.64E-06
Fe ²⁺	<<Cu ⁺	1.79E-09	
K ⁺			3.96E-03
Na ⁺	0.5 wt.% NaCl	8.56E-02	7.26E-02
Cu ⁺	Solubility	1.57E-05	
Ag ⁺	1000y	3.26E-07	
Au ⁺	1000y	3.09E-08	
HTe ⁻	1000y	7.37E-08	
Reference			Hedenquist 1990

References Cited

- Hedenquist, J.W. (1990) The thermal and geochemical structure of the Broadlands-Ohaaki geothermal system, New Zealand. *Geothermics*, 19, 151–185.
- Simmons, S.F., and Brown, K.L. (2006) Gold in magmatic hydrothermal solutions and the rapid formation of a giant ore deposit. *Science*, 314, 288–291.
- Simmons, S.F., and Brown, K.L. (2007) The flux of gold and related metals through a volcanic arc, Taupo Volcanic Zone, New Zealand. *Geology*, 35, 1099–1102.
- Simmons, S.F., Brown, K.L., and Tutolo, B.M. (2016) Hydrothermal transport of Ag, Au,

Cu, Pb, Te, Zn, and other metals and metalloids in New Zealand geothermal systems:
Spatial patterns, fluid-mineral equilibria, and implications for epithermal
mineralization. *Economic Geology*, 111, 589–618.